Available online at www.sciencedirect.com
ScienceDirect
Journal of the European Ceramic Society 29 (2009) 1125–1132
www.elsevier.com/locate/jeurceramsoc

Electrophoretic deposition of $La_{0.6}Sr_{0.4}Co_{0.8}Fe_{0.2}O_{3-\delta}$ cathodes on $Ce_{0.9}Gd_{0.1}O_{1.95}$ substrates for intermediate temperature solid oxide fuel cell (IT-SOFC)

M.J. Santillán [a], A. Caneiro [a], N. Quaranta [b], A.R. Boccaccini [c,*]

[a] *Comisión Nacional de Energía Atómica, CONICET, Centro Atómico Bariloche and Instituto Balseiro, 8400 S.C. de Bariloche, Argentina*
[b] *CIC Researcher, FR San Nicolás, Universidad Tecnológica Nacional, 2900 San Nicolás, Argentina*
[c] *Department of Materials, Imperial College London, Prince Consort Road, London SW7 2BP, UK*

Received 27 April 2008; received in revised form 24 July 2008; accepted 30 July 2008
Available online 13 September 2008

Abstract

Porous thick films of $La_{0.6}Sr_{0.4}Co_{0.8}Fe_{0.2}O_{3-\delta}$ (LSCF) on $Ce_{0.9}Gd_{0.1}O_{1.95}$ (CGO) substrates were prepared by the electrophoretic deposition (EPD) method. Organic suspensions of different compositions containing LSCF ceramic particles were investigated with the aim to determine the optimal composition of the suspension and EPD conditions. Stainless steel substrates were used in order to determine the optimal parameters for the EPD process. The best results were achieved with solutions containing acetylacetone, iodine and starch. The EPD conditions leading to uniform LSCF films were: applied voltage 20 V and deposition time 120 s, with the electrodes separated 1.5 cm. EPD was also demonstrated to be a simple and useful method for making porous LSCF cathodes on CGO substrates. It was shown that the microstructure of the films can be controlled by changing the applied voltage, deposition time and concentration of additives in suspension.

Keywords: Electrophoretic deposition; Solid oxide fuel cells; Porous cathodes

1. Introduction

Energy conversion using solid oxide fuel cells (SOFC) is a highly efficient and an environmentally friendly technology with reduced emission of pollutants in comparison to other power sources based on fossil fuel combustion.[1] However, the development of SOFC for efficient and low cost power generation has still failed to reach widespread commercial viability. This drawback is mainly due to thermal degradation problems associated with the high operation temperatures of SOFC and the need to use highly expensive materials. These issues have prompted the development of intermediate temperature SOFC (IT-SOFC), which will allow to use alternative interconnection materials and to achieve important cost reductions.[2] Since the operation at intermediate temperatures causes an increase in the interfacial polarization losses of a solid-state cell, the performance of IT-SOFC is strongly dependent on the cathode and cathode–electrolyte interface.

Optimizing IT-SOFC operation implies therefore the control of the microstructure of the cathode which depends on the deposition technique used for its fabrication. A convenient candidate for the cathode is the perovskite-type $La_{0.6}Sr_{0.4}Co_{0.8}Fe_{0.2}O_{3-\delta}$ (LSCF) material. This composition exhibits very good mixed ionic–electronic conductivity and it is appropriate for deposition on $Ce_{0.9}Gd_{0.1}O_{1.95}$ (CGO) electrolytes exhibiting a similar thermal expansion coefficient (TEC) than that of the CGO electrolyte.[3–5]

For IT-SOFC cathode preparation, various methods have been reported, such as laser assisted deposition,[6] chemical vapour deposition,[7] dip coating,[8] and spray coating.[9]

In the last years, electrophoretic deposition (EPD) has become an attractive technique for the fabrication of SOFC

* Corresponding author.
E-mail address: a.boccaccini@imperial.ac.uk (A.R. Boccaccini).

0955-2219/$ – see front matter © 2008 Elsevier Ltd. All rights reserved.
doi:10.1016/j.jeurceramsoc.2008.07.057

components.[10–14] EPD is a very effective process to produce thick films and free standing objects from suspensions of particles.[15] EPD is a two-step process, in the first step (electrophoresis), charged ceramic particles suspended in a liquid solvent are forced to move towards an electrode with opposite charge by applying an electric field. The second step (deposition) is the coagulation of the migrated particles onto the substrate to yield a deposit.[16] Like in all particle processing methods, in order to obtain a ceramic film with homogeneous and reproducible microstructure it is essential to control the particle packing in the green body and the sintering condition. EPD presents several advantages (short production times, low cost) and allows production of ceramic components and coatings of relevant quality in terms of controllable porosity, thickness and surface roughness.[15,16] Another fundamental characteristic of EPD coatings is that they can be made of any macroscopic shape, e.g. planar or tubular, because this depends only on the shape of the deposition substrate.[15]

The purpose of this study is to explore the potential application of the EPD technique for fabrication of $La_{0.6}Sr_{0.4}Co_{0.8}Fe_{0.2}O_{3-\delta}$ IT-SOFC cathodes with controlled microstructure on dense CGO substrates. To the best of our knowledge this is the first report on the use of the EPD technique for deposition of LSCF materials on CGO substrates.

2. Experimental procedures

2.1. Starting materials

Powders of $La_{0.6}Sr_{0.4}Co_{0.8}Fe_{0.2}O_{3-\delta}$ composition were prepared by the liquid-mix method (modified citrate route).[17] $SrCO_3$, La_2O_3, Co_3O_4 and metallic Fe were used as starting materials. Appropriate quantities were dissolved in a nitric acid solution and heated until the solvent evaporated and a light-red colored solid appeared. The mixture of nitrates was dissolved in a solution containing concentrated citric acid (99.9% $C_6H_8O_7$) in distillated water. Then, 2% of ethylene glycol ($C_2H_6O_2$) was added to this solution and a brown colored resin was obtained upon drying at 150 °C. The obtained product was heat treated at 800 and 950 °C in air for a period of 12 h. The presence of single phase materials was confirmed by powder XRD.

2.2. Preparation of suspensions for EPD

Acetylacetone, ethyl alcohol and acetone (High Purity Chemical) were used as solvents and poly(vinylbutyral-co-vinyl alcohol-co-vinyl acetate) (average Mw = 50000, Aldrich) (PVB), phosphate ester (PE) (Merck) as binder and dispersant, respectively. Iodine (Merck) was selected in order to enhance the charge of the particles in the acetone solutions. The suspensions utilized for EPD are listed in Table 1. The concentrations of components, including iodine, in the optimized suspensions finally used for EPD are also indicated in Table 1. These concentrations were determined by a trial-and-error approach, as discussed in Section 3 below. The concentrations of additives, such as PVB (binder) and PE (dispersant), were determined following the work of Zhitomirsky and Petric[12] on similar alcohol based suspensions. In all cases, the suspensions were ultrasonically treated before deposition.

2.3. Substrates for electrophoretic deposition

2.3.1. Stainless steel substrates

In order to determine the optimum deposition parameters, preliminary experiments were carried out on planar AISI 318 stainless-steel (SS) substrates of 15 mm × 10 mm × 0.5 mm. Before EPD, the substrates were cleaned with acetone.

2.3.2. CGO substrates

Dense solid electrolyte substrates were obtained by uniaxial pressing $Ce_{0.9}Gd_{0.1}O_{1.95}$ (CGO) powder (Praxair Surface Technologies). Green pellets of 13 mm in diameter and 1.1 mm thickness were sintered at 1360 °C for 6 h in air. Before deposition of the perovskite film by EPD, the surface of the samples was polished by conventional methods and covered with a thin film of gold or silver by sputtering. There is information in the specialized literature indicating that layers or particles of Ag on SOFCs substrates do not negatively affect the performance of the electrolyte.[18,19]

2.4. Electrophoretic deposition

2.4.1. Deposition on SS substrates

LSCF films were deposited on one face of the stainless steel substrates using LSCF suspension with compositions shown in Table 1. The EPD experiments were performed at constant voltage conditions (10–40 V) for periods between 60 and 300 s. At least three EPD experiments were carried out for each condition and the results were averaged. After deposition, the samples were dried at room temperature using a desiccator with controlled humidity.

2.4.2. Deposition on CGO substrates

EPD was carried out according to the optimal conditions determined on SS substrates. For deposition on CGO substrates, the EPD cell included the CGO electrode centered between two parallel planar stainless-steel counter-electrodes separated a distance of 1.5 cm, as shown in Fig. 1. This configuration allows the deposition of LSCF on both faces of the pellet simultaneously. Starch and graphite with different concentrations were also used in order to enhance the porosity of the LSCF film. Different amounts of starch, graphite and different deposition conditions were investigated such as deposition time (1–5 min) and voltage (20–40 V). Table 1 shows the concentrations of different suspensions investigated. Details of the different experiments conducted are given in the following sections. After EPD, the ceramic pellets were heat-treated at temperatures between 900 and 1100 °C in air for 2 h to sinter the LSCF layer and in order to promote adhesion of the LSCF coating on the CGO substrate.

Table 1
Composition of the suspensions employed in the EPD process of LSCF particles

Suspension	Solvent	LSCF (wt%)	I_2 (wt%)	Starch (wt‰)	Graphite (wt%)	PVB (wt%)	PE (wt%)
A	Ethanol	1.26	–	–	–	–	–
B		1.26	0.75	–	–	–	–
C		1.26	–	–	–	0.25	0.25
D	Acetone	1.28	–	–	–	–	–
E		1.28	0.77	–	–	–	–
F	Acetylacetone	1.05	0.63	0.1	–	–	–
G		1.05	0.63	0.52	0.2	–	–

2.5. Characterization techniques

The microstructure of the films was observed by scanning electron microscopy (SEM) using a Philips 515 microscope and the chemical composition verified by EDS using an EDAX Genesis 2000 spectrometer. Sintered films were characterized by X-ray diffraction (XRD) analysis with a Phillips PW 1700 diffractometer equipped with a graphite monochromator and Cu Kα radiation. The patterns were collected in the 20–70° 2θ range with scan steps of 0.02°.

3. Results and discussion

3.1. EPD on SS substrates

Different solvents were considered and their effects on the suspension stability were investigated. Table 1 gives an overview of the different suspensions investigated. The stability of the LSCF suspension depends mainly on the functional groups of the solvents and on the interaction between the ceramic particles, solvent and additives. The obtention of a homogeneous ceramic film by EPD requires a well dispersed and stable colloidal suspension. Consequently, the selection of the solvent plays a fundamental role in the development of suitable suspensions for EPD.

The results of the LSCF deposited weight (DW) per unit area as function of time for an applied voltage of 20 V are shown in Fig. 2. It can be seen that for all suspensions the DW of LSCF increases with time at a constant applied voltage. A low DW was obtained for a suspension containing pure ethanol and no additives (suspension A). It was also observed that the addition of iodine, PE and PVB to ethanol did not affect appreciably the DW, e.g. suspensions B and C, respectively.

The films obtained using alcoholic suspensions (A, B and C) showed poor adherence to the substrate and they did not cover the substrate's entire surface. Similar results were obtained using suspensions containing acetone and iodine (suspension E). In addition, it was also confirmed that deposition was not possible with suspensions containing only acetone (suspension D).

The DW was seen to increase appreciably when acetylacetone was used as solvent and I_2 as additive (suspension F). The shape of the curve shows a decreasing deposition rate at higher deposition times. This behavior is typical of a deposition pro-

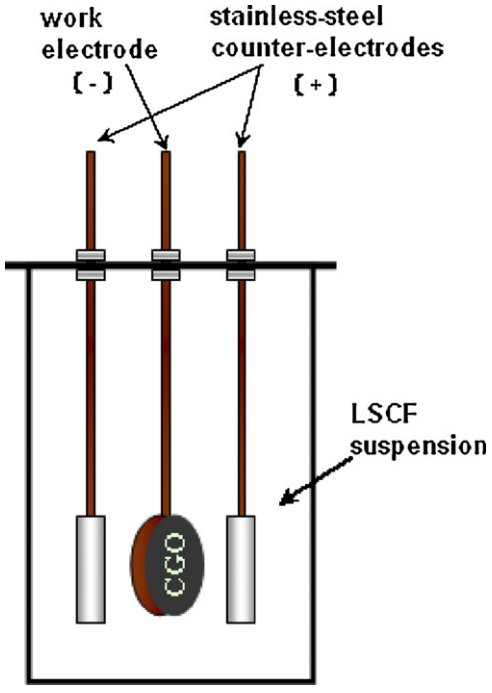

Fig. 1. Schematic diagram of EPD cell used for deposition of LSCF onto CGO disk substrates, where deposition occurs simultaneously on both faces of the CGO disk.

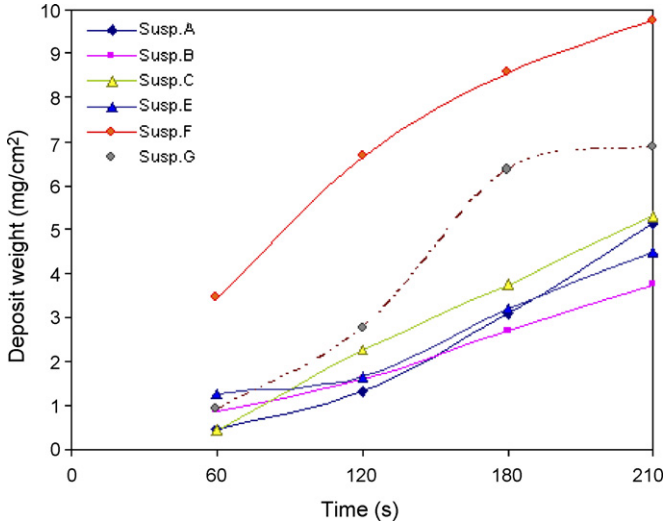

Fig. 2. Deposit weight vs. deposition time for different LSCF suspensions (see Table 1), all were deposited at 20 V.

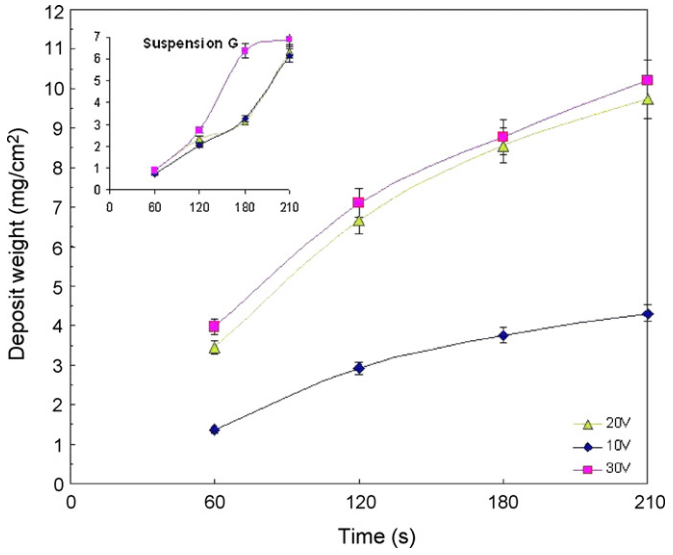

Fig. 3. Plot of deposit weight vs. deposition time obtained at different voltages (10, 20 and 30 V) from LSCF suspensions F and G, using AcAc as solvent. Data shown are average and standard deviation of three EPD runs for each condition.

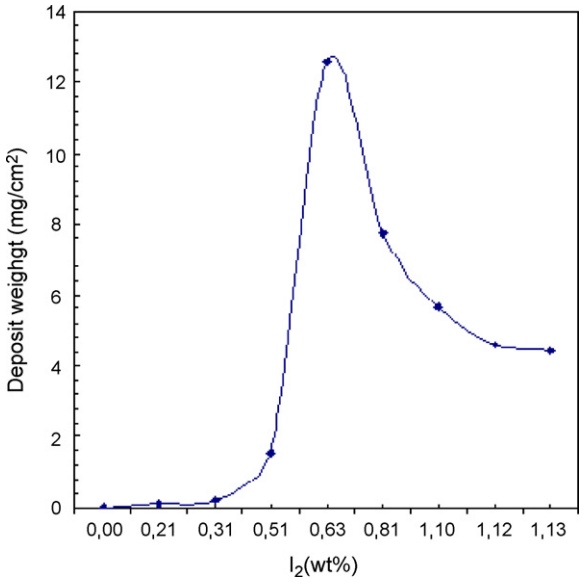

Fig. 4. Plot of LSCF weight deposited vs. iodine concentration added, using acetylacetone as solvent. The EPD process was carried out at 20 V for 120 s.

cess at constant voltage, as discussed in the literature.[15,16] This effect is due to the increment of the resistance between electrodes caused by both the growth of the film and by a decreasing concentration of the charge carrier in the solution as the EPD process progresses.[20]

Finally it was observed that the DW for suspension G showed intermediate values between those of suspension F and those of suspensions A, B, C and D. Suspension G contains, in addition to iodine, graphite and starch. These two additives were added with the aim of increasing the porosity of the deposited LSCF film after heat treatment. Taking into account that the better DW behaviour was achieved with suspensions F and G, only results obtained using these two suspensions will be reported and discussed further here.

The effect of the applied voltage (10, 20 and 30 V) on DW for suspensions F and G is shown in Fig. 3. It can be seen that the applied voltage has an appreciably effect on the DW for values between 10 and 20 V and that DW does not increase substantially for higher voltages. The effect is quite different for suspension G, where the DW does not change between 10 and 20 V but increases in the range 20–30 V.

It is well known that the amount of deposited material in EPD strongly depends on the nature of additives since they play a fundamental role on the stabilization of the suspension and on the surface charge of the ceramic particles. In the overall behaviour of particles in suspension the role of both adsorbed ions and steric stabilization must be considered.[12,16] In the present study the charge of the particles in suspension was promoted by proton adsorption on their surfaces.

Fig. 4 shows a plot of DW obtained at 20 V after 120 s as a function of the amount of iodine for a suspension containing 1.05 wt% of LSCF in acetylacetone (AcAc). A rapid increase of DW is observed for suspensions with iodine concentration in the range of ≈0.30 wt‰ to ≈0.63 wt‰. For higher values of iodine concentration, the DW decreases.

The next equation indicates the equilibrium reaction between AcAc and iodine to generate H^+ in the solution:

$$CH_3CH_2COCH_2COCH_2CH_3 + 2I_2 \leftrightarrow ICH_2CH_2COCH_2COCH_2CH_2I + 2I^- + 2H^+ \quad (1)$$

According to this reaction, a concentration of ≈0.30 wt‰ iodine is the minimum amount of iodine required to stabilize the ceramic particles in the suspension due to absorbed H^+ on their surface. This positive surface charge promotes the migration of the particles to the cathode under an external applied voltage. The maximum of iodine concentration at ≈0.63 wt‰ corresponds to the maximum surface charge achievable on the ceramic particles. For iodine concentrations higher than this maximum value, an excess of free H^+ of high mobility is produced in the suspension, which migrates to the cathode faster than the LSCF particles. The presence of H^+ near the cathode hampers the deposition of the arriving charged LSCF particles. As a consequence of this effect, the deposition weight decreases. A similar mechanism has been proposed in the literature for discussing the deposition of YSZ and TiO_2 films by EPD on different substrates,[10,21,22] however further work seems to be required on the electrochemistry of the system to consider the charge balance optimization in the suspension. The rate of migration of a charged species can be calculated by the following expression[23]:

$$y = \frac{zE}{6\eta r} \quad (2)$$

where E is the applied electric field, η the viscosity of the suspension, r the radius and z the charge of the particles. The z/r ratio for H^+ is much higher than that of the charged LSCF particles and consequently the mobility of H^+ in suspension is higher. Therefore, the presence of free H^+ with higher mobility than that of the LSCF particles will lead to a decrease of the amount of

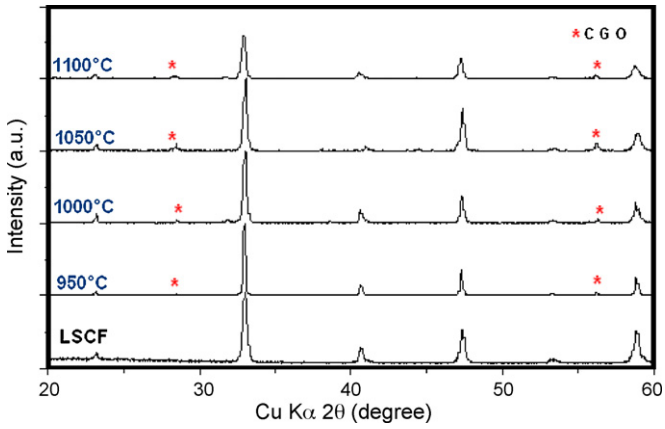

Fig. 5. XRD patterns of the LSCF films deposited on CGO substrates sintered at different temperatures (950–1100 °C) for 2 h.

LSCF deposited on the electrode, explaining the experimental results plotted in Fig. 3.

3.2. EPD of LSCF on dense CGO substrates

EPD of LSCF was performed on dense CGO pellets using suspension F (1.05 wt% LSCF, 0.63 wt‰ iodine and 0.1 wt‰ starch in AcAc). The deposition conditions (voltage and deposition time) were the same as those used for SS substrates. After EPD, the LSCF deposits on CGO substrates were heated at temperatures between 950 and 1100 °C during 2 h and the obtained films were characterised by XRD analysis. The XRD results for different sintering temperatures are shown in Fig. 5. It can be seen that the most intense reflexions are those of LSCF and the weaker peaks (labeled with *) correspond to the CGO substrate plotted in Fig. 4. No secondary crystalline phases due to possible chemical reactions between LSCF and CGO were detected at least under the detection limit of XRD. In fact, XRD is the technique being used to assess the formation of new crystalline phases following interface reactions in similar materials, as reported for example for LSCF layers on CGO and YSZ and for LSCF on composite electrolytes.[24,25]

3.3. Morphology of the LSCF films: Control of the microstructure

The morphology of electrophoretically deposited LSCF thick films was observed by SEM for different EPD conditions. SEM micrographs of the top surface of LSCF films obtained using suspension F at deposition times of 60, 120 and 180 s and voltages of 10, 20 and 30 V are shown in Fig. 6(a–i). The films were heat treated at 950 °C during 2 h in air. The most uniform films are seen to be those obtained under an applied voltage of 20 V (Fig. 6b, e and h). Those deposited at 10 and 30 V presented a rough surface. For low deposition voltage (10 V) (Fig. 6a, d and g), it is likely that the electrophoretic mobility of the particles is too low which usually leads to poor deposition rates. This in turn may have an effect on the homogeneity of the deposition. For higher applied voltages (30 V) (Fig. 6c, f and i), and therefore higher electric fields, turbulence could occur in the suspension which can affect the uniform flow of particles arriving to the electrode. Due to their high electrophoretic mobility and high deposition rate, a close-packed arrangement of the particles cannot be obtained and as a consequence of that, a rough and non-uniform deposit is obtained. Previous investigations have

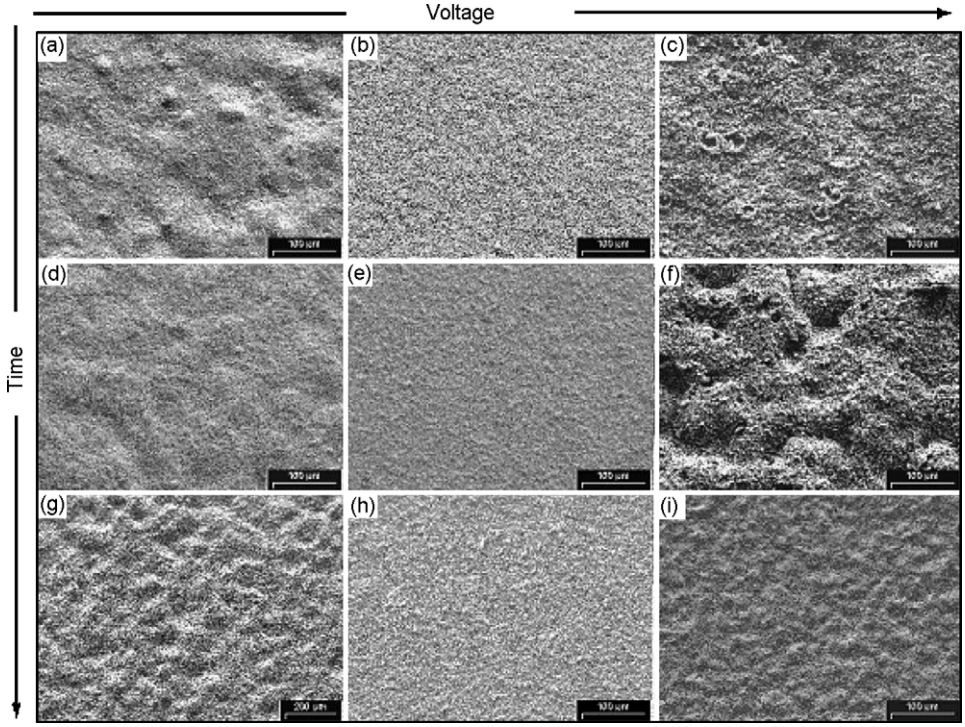

Fig. 6. SEM micrographs of LSCF films on CGO substrates heat-treated at 950 °C for 2 h in air. The EPD process was carried out using constant voltage of 10, 20 or 30 V during 60, 120 and 180 s from AcAc suspension containing 1.05 wt% of LSCF (suspension F).

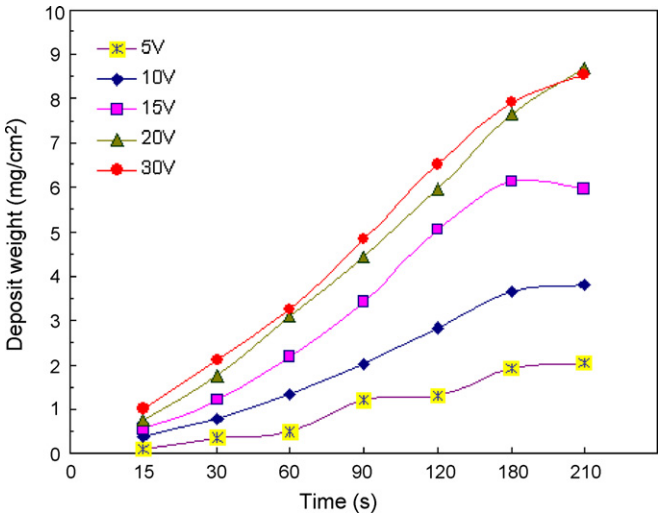

Fig. 7. Plot of LSCF deposit weight on GCO substrate vs. deposition time for EPD, carried out at different voltages and deposition times (suspension F).

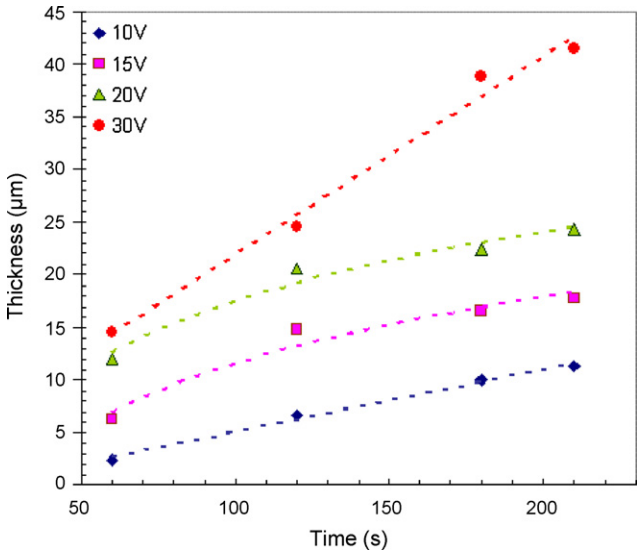

Fig. 8. Plot of the thickness of electrophoretically deposited LSCF films on GCO substrate vs. deposition time at different voltages and times.

shown similar behaviour.[10,26,27] Interestingly, our results confirm that there is an optimum voltage leading to deposits of uniform thickness, the deposition time being less important in its effect on deposition morphology (e.g. compare Fig. 6b, e and h).

The presence of large pores, shown in Fig. 6c, f and i, may be due to the departure of H^+ ions located near the substrate and between the particles. A high applied voltage increases the amount of hydrogen generated during deposition. This hydrogen leaves the cathode through the coating, originating pores inside the LSCF film, which are not eliminated by the subsequent heat treatment. A qualitative assessment of the SEM results confirms that, concerning the uniformity of the films, the best results were achieved at 20 V for a deposition time of 120 s (Fig. 6e).

Fig. 7 shows the variation of DW for LSCF deposits on CGO substrates at different voltages as a function of deposition time. It can be seen that the DW increases with deposition time. The higher deposition rates were achieved at 30 V since the rate of migration increases with the electric field, according to Eq. (2). Under this condition, it was observed that both the thickness and the porosity of the films increased with deposition time. The increase of porosity may be due to the evolution of hydrogen from the deposit during the electrophoretic deposition process.

The variation of the thickness of the films as function of deposition time for applied voltages of 10, 15, 20 and 30 V is shown in Fig. 8. The film thickness is seen to increase moderately with increasing deposition time for applied voltages of 10, 15 and 20 V. Under these deposition conditions, the thickness mainly increases for short deposition times (<100 s) and it seems to reach a saturation value for longer times. The reason for this behavior may be due to the growth of the film and the related decrease of the concentration of the suspension, as indicated above and well-known from the literature.[20] The thickness of the deposit increases appreciably with deposition time for applied voltage of 30 V. The increase of thickness at 30 V compared with that obtained at 20 V at similar DW clearly indicates also

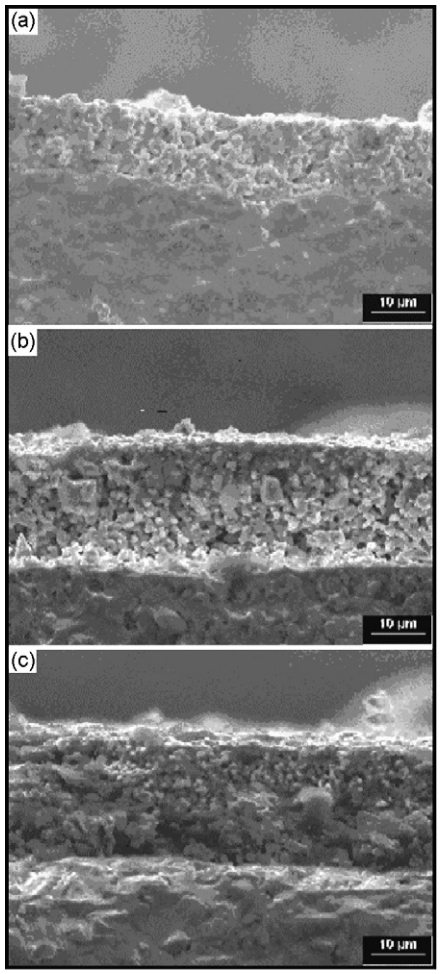

Fig. 9. Cross sections of LSCF films on CGO substrates obtained by EPD using suspension F (1.05 wt% LSCF in AcAc) at 20 V and deposition time of (a) 60 s, (b) 120 s and (c) 180 s.

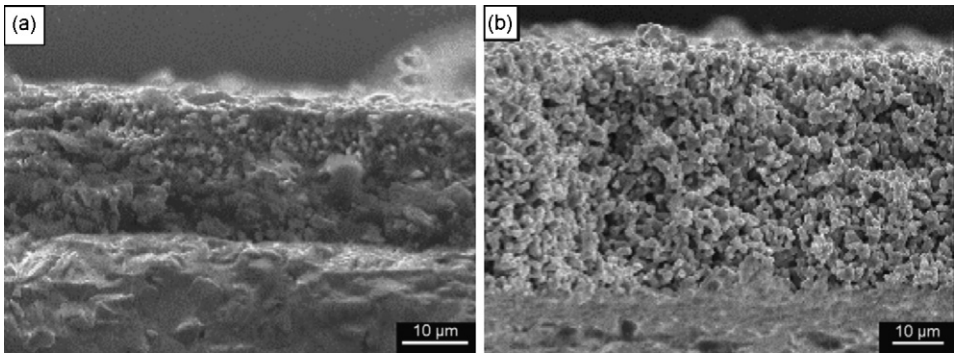

Fig. 10. Cross sections of LSCF films on CGO substrates obtained by EPD from suspension F (1.05%wt LSCF in AcAc) at (a) 20 V and (b) 30 V for deposition time of 180 s.

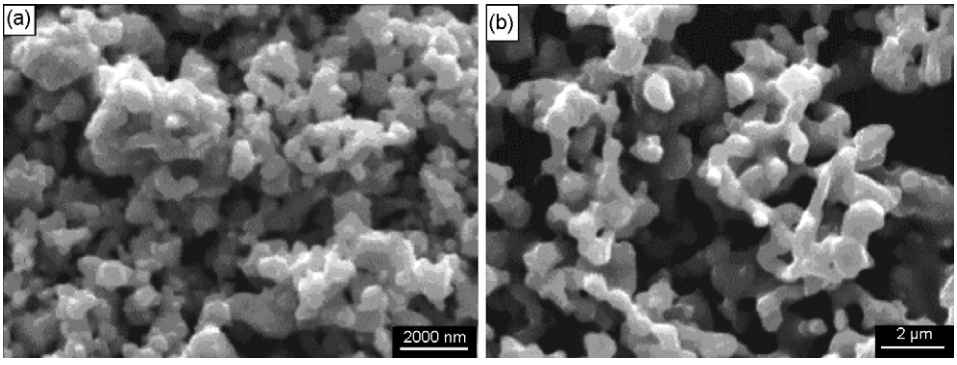

Fig. 11. Top view of SEM micrographs of LSCF films on CGO substrate obtained using (a) suspension F and (b) suspension G by EPD at 30 V–4 min.

a higher porosity for the films obtained at 30 V. This effect may be caused by the evolution of hydrogen from the films during the deposition process, as mentioned above.

SEM images showing the film thickness deposited at 20 V for three different deposition times are shown in Fig. 9. At this voltage the thickness of the films does not seem to vary appreciably with deposition time. Qualitatively, a good adherence between the film and substrate was observed in all cases when preparing the samples for SEM. The thickness of the film increases appreciably for an increment of the voltage from 20 to 30 V regardless similar DW and deposition time, as shown in Fig. 10. Similar results were obtained for EPD of YSZ, TiO_2 and carbon nanotubes films on metallic and ceramic substrates, as reported by several authors.[13,21,22,28,29]

3.4. LSCF cathodes with improved porosity

The effect of additions such as starch and graphite particles to suspension F (forming suspension G) was investigated in a preliminary study in this work in order to develop porous films. The objective of this part of the investigation was to assess if the EPD suspensions developed for dense films could be used also, with suitable additives, to fabricate porous LSCF layers. The concentration of starch was varied between 0.1 and 0.52 wt‰ while that of graphite was up to 0.2 wt%. The use of these additives should increase the porosity of the films due to the combustion of starch and graphite during the heat treatment sintering of the films post EPD.[30,31] The release of gases generated during the combustion process, such as CO_2 and H_2, contributes to porosity formation. In this case the EPD process was carried out at an applied voltage of 30 V for 2–5 min. The heat treatment was the same previously discussed. SEM observations of heat-treated samples revealed the presence of a large number of superficial pores. The amount of cracks and porosity and the thickness were found to increase with deposition time. Fig. 11a and b show the top view of films obtained from suspensions F and G at 30 V and deposition time 3 min, respectively. A higher porosity is present in the film obtained from suspension G, as expected. These results confirm the successful preliminary EPD approach developed here for production of porous LSCF films. However a more comprehensive investigation should be carried out to identify the optimum concentration of starch and carbon in the EPD suspension to achieve the required porosity.

4. Conclusions

A study of LSCF deposition onto metallic substrates by EPD was carried out in order to determine the optimal composition of the suspension and to determine the deposition parameters. A suspension based on acetylacetone and addition of iodine was found to be the most appropriate for LSCF deposition. For these conditions, the optimal iodine concentration (0.63 wt‰) for obtaining the highest deposition rate was determined. The EPD conditions leading to uniform LSCF films were: applied voltage 20 V and deposition time 120 s, with the

electrodes separated 1.5 cm. The effect of the applied voltage and deposition time on the morphology, porosity, and thickness of LSCF films onto CGO substrate was evaluated and discussed. It was found that a high applied voltage (30 V) increases the porosity and the thickness of the film. Similar effect was obtained with addition of starch and graphite particles to the organic suspension. Thus EPD was confirmed to be a convenient and simple technique to obtain porous thick LSCF films on CGO substrates with controlled microstructure. The composition of the suspension, applied voltage and deposition time, as investigated here, are the key parameters playing a crucial role in determining the microstructure of the electrophoretically deposited films. Current work focuses on characterizing the electrochemical properties of the new LSCF layers.

Acknowledgements

The authors thank Carlos Cotaro, Ernesto Scerbo and Silvina Perez Fornells (CAB-IB) for assistance with SEM, EDS and XRD analyses. Financial support from CNEA, SECyT (ANPCyT PICT 12-14493), CONICET (PIP 5594), and UNCuyo (PI + D 06/C183) is acknowledged.

References

1. Chung, T-D., Hong, W-T., Chyou, Y-P., Yu, D-D., Lin, K-F. and Lee, C-H., Efficiency analyses of solid oxide fuel cell power plant systems. *Appl. Thermal Eng.*, 2008, **28**, 933–941.
2. Yin, Y., Li, S., Xi, C. and Meng, G., Electrochemical performance of IT-SOFCs with a double-layer anode. *J. Power Sources*, 2007, **167**, 90–93.
3. Inaba, H. and Tagawa, H., Ceria-based solid electrolytes. *Solid State Ionics*, 1996, **83**, 1–16.
4. Steele, B. C. H., Materials for IT-SOFC stacks 35 years R&D: the inevitability of gradualness? *Solid State Ionics*, 2000, **134**, 3–20.
5. Grunbaum, N., Dessemond, L., Fouletier, J., Prado, F. and Caneiro, A., Electrode reaction of $Sr_{1-x}La_xCo_{0.8}Fe_{0.2}O_{3-\delta}$ with x = 0. 1 and 0. 6 on $Ce_{0.9}Gd_{0.1}O_{1.95}$ at $600 \leq T \leq 800^{\circ}C$. *Solid State Ionics*, 2006, **177**, 907–913.
6. Imanishi, N., Matsumura, T., Sumiya, Y., Yoshimura, K., Hirano, A., Takeda, Y. *et al.*, Impedance spectroscopy of perovskite air electrodes for SOFC prepared by laser ablation method. *Solid State Ionics*, 2004, **174**, 245–252.
7. Takeyama, T., Takahashi, N., Nakamura, T. and Itoh, S., δ-Bi_2O_3 thin films deposited on dense YSZ substrates by CVD method under atmospheric pressure for intermediate temperature SOFC applications. *Surf. Coat. Technol.*, 2006, **200**, 4797–4801.
8. Baqué, L. and Serquis, A., Microstructural characterization of $La_{0.4}Sr_{0.6}Co_{0.8}Fe_{0.2}O_{3-\delta}$ films deposited by dip coating. *Appl. Surf. Sci.*, 2007, **254**, 213–218.
9. Baqué, L., Serquis, A., Grunbaum, N., Prado, F. and Caneiro, A., Preparation and characterization of solid oxide fuel cells cathode films. *Mater. Res. Soc. Symp. Proc.*, 2006, **928**, 181–186.
10. Ishihara, T., Sato, K. and Takita, Y., Electrophoretic deposition of Y_2O_3-stabilized ZrO_2 electrolyte films in solid oxide fuel cells. *J. Am. Ceram. Soc.*, 1996, **79**, 913–919.
11. Zhitomirsky, I. and Petric, A., Electrolytic and electrophoretic deposition of CeO_2 films. *Mater. Lett.*, 1999, **40**, 263–268.
12. Zhitomirsky, I. and Petric, A., Electrophoretic deposition of ceramic materials for fuel cell applications. *J. Eur. Ceram. Soc.*, 2000, **20**, 2055–2061.
13. Matsuda, M., Hosomi, T., Murata, K., Fukui, T. and Miyake, M., Fabrication of bilayered YSZ/SDC electrolyte film by electrophoretic deposition for reduced-temperature operating anode-supported SOFC. *J. Power Sources*, 2007, **165**, 102–107.
14. Negishi, H., Oshima, N., Sakaki, K., Haraya, K., Idemoto, Y., Koura, N. *et al.*, Preparation of tubular mixed conducting oxide membrane by electrophoretic deposition technique. *Desalination*, 2006, **200**, 71–73.
15. Boccaccini, A. R. and Zhitomirsky, I., Application of electrophoretic and electrolytic deposition techniques in ceramics processing. *Curr. Opin. Solid State Mater Sci.*, 2002, **6**, 251–260.
16. Sarkar, P. and Nicholson, P. S., Electrophoretic deposition (EPD): mechanisms, kinetics, and application to ceramics. *J. Am. Ceram Soc.*, 1996, **79**, 1987–2002.
17. Serquis, A., Prado, F. and Caneiro, A., Synthesis method, control of cationic composition and superconducting behavior of $Nb_{1.85}Ce_{0.15}Cu_{1\pm\delta}O_y$. *Phys. C*, 1995, **253**, 339–350.
18. Wang, S., Kato, T., Nagata, S., Honda, H., Kaneko, T., Iwashita, N. *et al.*, Performance of a $La_{0.6}Sr_{0.4}Co_{0.8}Fe_{0.2}O_3$–$Ce_{0.8}Gd_{0.2}O_{1.9}$–Ag cathode for ceria electrolyte SOFCs. *Solid State Ionics*, 2002, **146**, 203–210.
19. Simner, S. P., Anderson, M. D., Templeton, J. W. and Stevenson, J. W., Silver-perovskite composite SOFC cathodes processed via mechanofusion. *J. Power Sources*, 2007, **168**, 236–239.
20. Anné, G., Vanmensel, K. and Van der Biest, O., Influence of the suspension composition on the electric field and deposition rate during electrophoretic deposition. *Colloids Surf. A Physicochem. Eng. Aspects*, 2004, **245**, 35–39.
21. Kaya, C., Kaya, F., Su, B., Thomas, B. and Boccaccini, A. R., Structural and functional thick ceramic coatings by electrophoretic deposition. *Surf. Coat. Technol.*, 2005, **191**, 303–310.
22. Santillán, M. J., Quaranta, N. E., Membrives, F. and Boccaccini, A. R., Characterization of TiO_2 nanoparticle suspensions for electrophoretic deposition. *J. Nanopart. Res.*, 2008, **10**, 787–793.
23. Ferrari, B. and Moreno, R., Electrophoretic deposition of aqueous alumina slips. *J. Eur. Ceram. Soc.*, 1997, **17**(4), 549–556.
24. Murray, E. P., Sever, M. J. and Barnett, S. A., Electrochemical performance of (La,Sr)(Co,Fe)O_3–(Ce,Gd)O_3 composite cathodes. *Solid State Ionics*, 2002, **148**, 27–34.
25. Guo, W., Liua, J., Jin, C., Gao, H. and Zhanga, Y., Electrochemical evaluation of $La_{0.6}Sr_{0.4}Co_{0.8}Fe_{0.2}O_{3-I}$–$La_{0.9}Sr_{0.1}Ga_{0.8}Mg_{0.2}O_{3-I}$ composite cathodes for $La_{0.9}Sr_{0.1}Ga_{0.8}Mg_{0.2}O_{3-t}$ electrolyte SOFCs. *J. Alloys Compd.*, 2008., doi:10.1016/j.jallcom.2008.05.058.
26. Zhitomirsky, I., Cathodic electrodeposition of ceramic and organoceramic materials. Fundamental aspects. *Adv. Colloid Interface Sci.*, 2002, **97**, 279–317.
27. Sarkar, P., De, D. and Rho, H., Synthesis and microstructural manipulation of ceramics by electrophoretic deposition. *J. Mater. Sci.*, 2004, **39**, 819–823.
28. Chicatún, F., Cho, J., Schaab, S., Brusatin, G., Colombo, V., Roether, J. A. *et al.*, Carbon nanotube deposits and CNT/SiO_2 composite coatings by electrophoretic deposition. *Adv. Appl. Ceram.*, 2007, **106**(4), 186–195.
29. Negishi, H., Sakai, N., Yamaji, K., Horita, T. and Yokokawa, H., Application of electrophoretic deposition technique to solid oxide fuel cells. *J. Electrochem. Soc.*, 2000, **147**, 1682–1687.
30. Yamaji, K., Kishimoto, H., Xiong, Y., Horita, T., Sakai, N. and Yokokawa, H., Performance of anode-supported SOFCs fabricated with EPD techniques. *Solid State Ionics*, 2004, **175**, 165–169.
31. Xu, Z., Rajaram, G., Sankar, J. and Pai, D., Electrophoretic deposition of YSZ electrolyte coatings for SOFCs. *Fuel Cells Bull.*, 2007, **3**, 12–16.